Author Manuscript

Author Manuscript

Author Manuscript

Author Manuscript

HHS Public Access

Author manuscript

Biochim Biophys Acta Mol Basis Dis. Author manuscript; available in PMC 2022 January 01.

Published in final edited form as:

Biochim Biophys Acta Mol Basis Dis. 2021 January 01; 1867(1): 165991. doi:10.1016/j.bbadis.2020.165991.

In-vivo imaging revealed antigen-directed gingival B10 infiltration in experimental periodontitis

Yufeng Wang[1,2], **Yang Hu**[2,3], **Keqing Pan**[2,4], **Hao Li**[2,5], **Shu Shang**[6], **Yuhua Wang**[1], **Guoyao Tang**[1], **Xiaozhe Han**[2,3]

[1]Department of Oral Medicine, Ninth People's Hospital, Shanghai Jiao Tong University School of Medicine; Shanghai Key Laboratory of Stomatology & Shanghai Research Institute of Stomatology; National Clinical Research Center of Stomatology, Shanghai 200011, China.

[2]Department of Immunology and Infectious Diseases, The Forsyth Institute, Harvard School of Dental Medicine Affiliate, Cambridge, MA 02142, United States.

[3]Department of Oral Medicine, Infection and Immunity, Harvard School of Dental Medicine, Boston, MA 02115, United States.

[4]Department of Stomatology, the affiliated hospital of Qingdao University, Qingdao, Shandong 266003, China.

[5]Department of Prosthodontics, the Affiliated Hospital of Stomatology, Guangxi Medical University, Nanning 530021, China.

[6]Shanghai University of Medicine and Health Sciences, Shanghai 201318, China.

Abstract

Our previous study demonstrated that IL-10 secreting B (B10) cells alleviate inflammation and bone loss in experimental periodontitis. The purpose of this study is to determine whether antigen-specificity is required for the local infiltration of B10 cells. Experimental periodontitis was induced in the recipient mice by placement of silk ligature with or without the presence of live *Porphyromonas gingivalis* (*P. gingivalis*). Donor mice were pre-immunized by intraperitoneal (IP) injection of formalin-fixed *P. gingivalis*, or PBS as non-immunized control. Spleen B cells were

[#]corresponding author: Xiaozhe Han, DMD., Ph.D., 245 First Street, Cambridge, MA 02142, Tel: (617) 892-8447; Fax: (617)892-8612; Xhan@forsyth.org.

Credit Author Statement

Authors' contributions: Y(Yufeng)W, contributed to conception and design, contributed to acquisition, analysis, and interpretation, drafted manuscript; YH, contributed to conception and design, contributed to acquisition, analysis, and interpretation, drafted manuscript, critically revised the manuscript for important intellectual content; KP, contributed to conception and design, contributed to acquisition, analysis, and interpretation; HL, contributed to acquisition, analysis, and interpretation; SS, contributed to acquisition, analysis, and interpretation; Y(Yuhua)W, critically revised the manuscript for important intellectual content; GT, critically revised the manuscript for important intellectual content; XH, contributed to conception and design, contributed to acquisition, analysis, and interpretation, critically revised the manuscript for important intellectual content, Agree to be accountable for all aspects of the work in ensuring that questions relating to the accuracy or integrity of any part of the work are appropriately investigated and resolved.

Publisher's Disclaimer: This is a PDF file of an unedited manuscript that has been accepted for publication. As a service to our customers we are providing this early version of the manuscript. The manuscript will undergo copyediting, typesetting, and review of the resulting proof before it is published in its final form. Please note that during the production process errors may be discovered which could affect the content, and all legal disclaimers that apply to the journal pertain.

Declaration of interests

The authors declare that they have no known competing financial interests or personal relationships that could have appeared to influence the work reported in this paper.

Author Manuscript Author Manuscript Author Manuscript Author Manuscript

purified and treated with LPS and CpG for 48 hours to expand the B10 population *in vitro*. Fluorescence-labeled B10 cells were transferred into the recipient mice by tail vein injection and were tracked on day 0, 3, 5 and 10 using IVIS Spectrum *in vivo* imaging system. The number of B10 cells and *P. gingivalis*-binding B cells were significantly increased after *in vitro* treatment of LPS and CpG. On day 5, the fluorescence intensity in gingival tissues was the highest in mice transferred with B10 cells from pre-immunized donor mice. Gingival expression of IL-6, TNF-α, RANKL/OPG ratio and periodontal bone loss in recipient mice were significantly reduced, and the expression of IL-10 and the number of CD19+ B cells were significantly increased after pre-immunized B10 cell transfer in the presence of antigen, compared to those with non-immunized B10 cell transfer or no antigen presence. This study suggests that antigen specificity dictate the local infiltration of B10 cells into periodontal tissue and these antigen-specific B10 cells promote anti-inflammatory responses.

Keywords

experimental periodontitis; B10 cells; in vivo imaging; antigen specificity

Introduction

IL-10-producing B (B10) cells have been the most studied regulatory B cell subset [1–3]. It has been shown to balance immune response during inflammation, autoimmunity and cancer [4, 5]. Inflammation and host immune response to periodontal microbiota are major characteristic changes elicited in periodontitis [6, 7]. Our recent studies indicated that adoptive transfer of B10 cells alleviate experimental periodontal bone loss *in vivo* [8]. In addition, local induction of B10 cells by *Porphyromonas gingivalis* (*P. gingivalis*) lipopolysaccharide (LPS) and cytosine-phospho-guanine (CpG) oligodeoxynucleotides can alleviate inflammation and bone loss in ligature-induced experimental periodontitis mouse model [9], indicating that local activation of B10 cells in gingival tissue can increase immune regulatory competence and suppress inflammatory response and related bone loss. Moreover, *in vitro* B10 cell activation by *P. gingivalis* LPS and CpG showed differences in expression of IL-10 in *P. gingivalis*-immunized vs. non-immunized mice B cells [10], suggesting that antigen priming may play an important role in B10 cell competence during the host immune response.

Although it was unequivocally demonstrated from our previous studies that adoptively transferred B10 cells can alleviate periodontal inflammation and bone loss [8], and B10 cell function can be induced locally in gingival tissues [9, 11], we have yet to demonstrate the direct evidence of local infiltration of B10 cells due to the difficulty of tracking adoptively transferred B cells and distinguishing endogenous vs. exogenous B cells. It is still unclear about the fate of those adoptively transferred B cells, and their dynamic trafficking from circulation into local gingival tissues. Therefore the question remains on how systemically originated B10 cells are recruited and directed into gingival tissues. Answering this question is important to clarify the mechanism by which activated B10 cells achieve local infiltration and is valuable for the design of future targeted therapeutic strategies.

Author Manuscript Author Manuscript Author Manuscript Author Manuscript

In the recent years, *in vivo* optical imaging approach using fluorescence and bioluminescence has shown promise for improved rapid analysis and imaging of cancer biology [12, 13], infectious diseases [14], and immune system functions [15]. It represents a new technology for comprehensively studying living organisms in a less invasive way [16–18]. While these techniques have been frequently employed to assessing cell trafficking in experimental tumor immunology [19], it has not been successfully applied to immune cell trafficking in periodontal disease, largely due to the limited accessibility and the complex anatomy of periodontium. New methods are needed to successfully visualize and quantify targeted cells with fluorescence or bioluminescence imaging over an extended period of time, in order to evaluate the process of dynamic immune cell migration and infiltration in periodontal tissue without euthanizing the experimental animals.

Additionally, our previous data showing that the local gingival induction of B10 cells with LPS and CpG may also involve activation of other type of immune cells in the gingival tissue such as T cells, macrophages, which secret IL-10 as well [9]. To clarify the role of B10 cells, we expanded the B10 cells with LPS and CpG *in vitro* and then adoptively transferred these cells through tail vein to recipient mice with experimental periodontitis. The data showed that transferring B10 cells from *P. gingivalis*-immunized mice can significantly reduce periodontal bone loss of recipient mice as compared to those recipient mice transferred with non-B10 cells [8]. However, the mechanism of the systemically-derived B10 cells function remains unclear. It is critical to understand whether the antigen specificity plays a key role in the local infiltration of activated B10 cells. Thus, the purpose of present study is to determine whether the antigen specificity is required to direct local infiltration of B10 cells using our newly established *in vivo* imaging system.

Material and Methods

Animal

Wild-type (WT) C57BL/6J mice of 8 weeks from Jackson laboratories were used. All mice were housed in specific pathogen-free units. All the experimental procedures were approved by the Institutional Animal Care and Use Committee of The Forsyth Institute.

Bacterial culture

The *P. gingivalis* (Strain ATCC 33277) were maintained on supplemented sterile blood agar containing 3.7% brain heart infusion agar (Sigma), 2% gelose, 0.001% menadione, 0.005% hemin, 0.05% cysteine, 5%–7% defibrinated sheep blood for 4–5 days and then transferred into complement brain-heart infusion medium containing 3.7% brain heart infusion agar, 0.001% menadione, 0.005% hemin, 0.05% cysteine for 48 h before use. Bacteria were grown in an anaerobic chamber (N_2 : CO_2 : H_2, 85 : 10 : 5) at 37°C.

Immunization of donor mice

Donor mice were initially pre-immunized with fixed *P. gingivalis* in PBS (5×10^8/mL, 200 μL) by intraperitoneal (IP) injection. Seven days later, the donors were further IP boosted with 10^7 fixed *P. gingivalis* for another 4 days before spleen B cell isolation. Non-

Author Manuscript Author Manuscript Author Manuscript Author Manuscript

immunized donors were treated with IP injection of sterilized PBS (200 μL) at the same time points.

Establishment of experimental periodontitis in recipient mice

WT recipient mice of 8 weeks old were fed with drinking water containing antibiotics (sulfamethoxazole and trimethoprim, 850μg/170μg per ml) for 3 days and then antibiotics-free water for 4 days. Meanwhile, these mice were also fed with fluorescence-free solid food. They were anesthetized on day 8 by IP injection of anesthetics. Sterilized silk ligature (size 6–0) with or without live *P. gingivalis* was placed subgingivally around the maxillary right second molar 3 days before B cell transfer. Un-ligatured left second molar was used as control. To better provide the antigen around periodontal lesion, 1×10^8 of live *P. gingivalis* in 1% carboxymethylcellulose (CMC) gel was inoculated daily around the maxillary right second molar for 3 days before B cell transfer. Fluorescence-free powder food was given after ligation till the end of the experiment.

Isolation and treatment of B cells

The donor mice were euthanized with carbon dioxide in a chamber. The spleens were extracted immediately and were grinded on a metal mesh to acquire single-cell suspension. The red blood cells were then lysed with Ammonium-Chloride-Potassium Lysing Buffer (Gibco). The splenocytes were then labelled with biotin-conjugated antibodies against CD4, CD11c, CD49b, CD90.2, Gr-1, and Ter-119 (Pan B isolation kit, Miltenyi Biotec). After incubation with anti-biotin antibody coupled magnetic beads, B cells were isolated without activation or stimulation by depleting the labelled cells (>98.5% purity). Isolated B cells were re-suspended to a concentration of 1×10^7 cells/mL, and were cultured in 6-well plates (2 mL/well) for 48 hours before transfer. B cells from pre-immunized donors were treated with cytosine-phospho-guanine (CpG, 1μM/mL) plus *P. gingivalis* lipopolysaccharide (*P. gingivalis* LPS, 1μg/mL) to expand the B10 population. B cells from non-immunized donors were cultured under same conditions without CpG and *P. gingivalis* LPS treatment. The cultured B cells from pre-immunized and non-immunized mice were stained with APC-labeled anti-mouse CD19 monoclonal antibody (Biolegend) and PE-Cy7-labeled anti-mouse IL-10 monoclonal antibody (Biolegend) for identification of the B10 population ($CD19^+IL\text{-}10^+$) by flow cytometry. Five hours before adoptive transfer, 50 ng/mL PMA (Sigma), 500 ng/mL ionomycin (Sigma), and 2 μM monensin (Biolegend) were added into the cell culture as previously described [8] to stop the cells from releasing the synthesized IL-10 proteins. For identifying the antigen specific B cell population (represented as the *P. gingivalis*-binding B cells), the cultured B cells were labelled with anti-CD19 antibody, and then were mixed (ratio 1:10) with propidium iodide (PI)-labelled fixed *P. gingivalis* on ice for 30 minutes. The *P. gingivalis*-binding B cells was recognized as $CD19^+PI^{lo/int}$ by flow cytometry.

Labelling and transfer of B cells

The cultured B cells were labelled with VivoTrack 680 (Perkin Elmer), a near-infrared water-soluble fluorescent agent for *in vivo* imaging. The cells were mixed with labelling agent (volume ratio 1:1) at room temperature and then were washed 3 times with complete IMDM medium. The cells were re-suspended in PBS and were protected from light before

Author Manuscript Author Manuscript Author Manuscript Author Manuscript

transfer. The B cell transfer was performed immediately after labelling. The recipient mice were prepared on a heating pad so that the tail vein could be enlarged and more visible. A plastic restraint was used to hold the mice, and 1×10^6 of labelled B cells in 100 μL of PBS was transferred by tail vein injection.

In vivo imaging

After B cell transfer, the recipient mice were stabilized facing up on a restrain plate with help of magnetic columns. Mouth opener device was used to keep the palatal area completely exposed to the detecting lens of the IVIS system. Masking material was placed around the lips and teeth to avoid the light reflection disturbance. The excitation wavelength was set at 480 nm while the emission wavelength was set at 680 nm. The exposure time was set to 0.5 second. After signal acquisition, the average fluorescence intensity was calculated. The time points of detection were day 0 (before transfer), day 3 (after transfer), day 5 and day 10.

Tissue histological analysis

Collected maxillae were fixed in 4% formaldehyde overnight followed by decalcification in 10% EDTA for 2 weeks at 4 °C with agitation. Paraffin-embedded specimens were cut in 5 μm thickness along the long axis of the molars. For immunohistochemistry staining, sections were de-paraffinized, rehydrated and incubated with 3% hydrogen peroxide for 10 min followed by heat induced antigen retrieval in 10 mM sodium citrate buffer at pH 6.0. After blocking with 1% BSA for 30 min at RT, tissue sections were incubated with rabbit anti-mouse IL-10 Ab (1:50, Abcam) or rabbit anti-mouse CD19 Ab (1:100, Abcam) for 1h at RT and were washed with TBST for three times. The alkaline phosphatase (AP) conjugated anti-rabbit IgG secondary antibody (ImmPRESS AP polymer detection kit, Vector) was used to visualize the positive staining according to the manufacturer's instruction. Images of nine randomly chosen fields from gingiva papilla to root apex between the second molar and adjacent molars were obtained and the number of positive cells was calculated.

Quantitative real-time PCR (qRT-PCR)

Total RNA from gingival tissue was extracted by using a PureLink RNA minikit (Life Technologies, Carlsbad, CA) according to the manufacturer's instructions. Isolated mRNA (0.1 μg each) was reverse transcribed into cDNA by using the SuperScript II reverse transcription system in the presence of random primers (Invitrogen). Real-time PCR was then carried out with a 20μl reaction mix by using a SuperScript II Platinum SYBR green two-step reverse transcription-quantitative PCR (RT-qPCR) kit (Life Technology) with a Roche LightCycler 480 instrument (Roche Diagnostics). The following primers were used: TNF-α forward 5'-CACAGAAAGCATGATCCGCGACGT-3'; TNF-α reverse 5'-CGGCAGAGAGGAGGTTGACTTTCT-3'; IL-1β forward 5'-CCAGCTTCAAATCTCACAGCAG-3'; IL-1β reverse 5'-CTTCTTTGGGTATTGCTTGGGATC-3'; IL-10 forward 5'-CTTCTTTGGGTATTGCTTGGGATC-3'; IL-10 reverse 5'-CAGCAGACTCAATACACACT-3'; RANKL forward 5'-GGGTGTGTACAAGACCC-3'; RANKL reverse 5'-CATGTGCCACTGAGAACCTTGAA-3''; OPG forward 5'-AGCAGGAGTGCAACCGCACC-3'; OPG reverse 5'-TTCCAGCTTGCACCACGCCG-3';

Author Manuscript Author Manuscript Author Manuscript Author Manuscript

IL-6 forward 5'-TCCAGTTGCCTTCTTGGGAC-3'; IL-6 reverse 5'-GTACTCCAGAAGACCAGAGG-3'; GAPDH forward AGCAGTCCCGTACACTGGCAAAC; GAPDH reverse TCTGTGGTGATGTAAATGTCCTCT.

Bone morphometric analysis

The maxillae were harvested and defleshed by a dermestid beetles colony. The maxillae was bleached with 3% hydrogen Peroxide then stained with 1% toluidine blue. Bone resorption measurements were used a Nikon microscope (Nikon SMZ745T, Nikon Instruments Inc, Janpan). Images of palatal surfaces of maxillae were pictured and bone loss polygonal area were examined using Image J software (NIH). The area was formed by longitudinally from the cementoenamel junction (CEJ) to the alveolar bone crest (ABC), transversely from the distal of the first maxillary molar to the mesial of the third maxillary molar. All the area results were presented in mm^2.

Statistical analysis

The intensity of *in vivo* fluorescence was calculated by the imaging software of the system. An average intensity was calculated and analyzed with a non-parametric test (Mann-Whitney test). Unpaired-T-test was used to evaluate the difference among two groups. Data analysis was processed using GraphPad Prism (version 8). $P < 0.05$ was considered statistically significant.

Results:

The populations of B10 cells and antigen-specific B cells were increased after treatment with LPS and CpG *in vitro*.

In the flow cytometry analysis, B10 cells were gated as $CD19^{+}IL\text{-}10^{+}$ cells, while the antigen-specific (*P. gingivalis* binding) B cells were gated as $CD19^{hi}PI^{lo/int}$ cells. After 48h *in vitro* treatment of CpG (1μM/mL) plus *P. gingivalis*-LPS (1μg/mL), the population of B10 cells increased significantly in the treated group compared with untreated group, from 2.95% ±0.61% to 9.92%±1.90% (Fig. 1A, 1B). Meanwhile, the percentage of antigen-specific *P. gingivalis* binding B cells was initially less than 1% (0.23%±0.05%) and was increased to 8.12%±0.50% after treatment (Fig.1C, 1D). Taken together, B cells from *P. gingivalis*-immunized mice showed high antigen-specificity and IL-10 production capacity after CpG + *P. gingivalis*-LPS stimulation.

Fluorescence signal from labelled cells was detectable and stable *in vitro* and *in vivo*.

The labelled cells were cultured *in vitro* to determine the duration and intensity of the fluorescence signal. The unlabeled cells showed no fluorescence at the preset excitation wavelength. However, the fluorescence signal was detectable for about 10 days and faded gradually in labelled cells (Fig. 2A). The intensity of fluorescence was positively correlated with the number of cells, while it was inversely related to the culture time *in vitro*. The positioning of the animal and the focusing of image acquisition on oral cavity of the animal in IVIS Spectrum *in vivo* imaging system were shown in Figure. 2B. The fluorescence signal was detected in gingival tissue after the sub-gingival injection of labelled B cells (Fig.

Author Manuscript Author Manuscript Author Manuscript Author Manuscript

2C) and was analyzed quantitatively (Fig. 2D). It showed that the fluorescence signal could be readily detected for more than 10 days. According to the timeline, day 3 and day 5 after transfer could be the best time points to visualize the presence of labelled cells (Fig. 2D). These results strongly substantiated the feasibility of the present study, demonstrating the detectability of transferred cells in periodontal area *in vivo,* and the duration sufficient for longitudinal observation.

Antigen-specific B cells infiltrated into inflamed gingival tissue more effectively and lasted longer than non-specific B cells.

The recipient mice were divided into 4 groups. Group A was ligated with the silk ligature without live *P. gingivalis* and transferred with non-immunized B cells (ligation + non-immunized B cells). Group B was ligated with silk ligature without live *P. gingivalis* and transferred with pre-immunized B cells (ligation + pre-immunized B cells); Group C was ligated with silk ligature with live *P. gingivalis* and transferred with non-immunized B cells (*P. gingivalis* ligation + non-immunized B cells); Group D was ligated with the silk ligature with live *P. gingivalis* and transferred with pre-immunized B cells (*P. gingivalis* ligation + pre-immunized B cells); Each group included 5 recipients and received 1×10^6 of labelled B cells by tail vein injection, respectively. The fluorescence signal was measured before B cell transfer, day 3 after transfer, day 5 and day 10 accordingly.

On day 3 (Fig. 3C, 3D), the intensity of fluorescence in group D (3.36×107 ± 0.29×106 [p/s/cm^{2}sr] / [μW/cm^2]) was significantly higher than that in Group A (2.66×107 ± 0.18×106, $p<0.01$). It's indicated that the transferred antigen-specific B cells could be recruited more efficiently when antigen is present. It is noted that there is an increased infiltration by pre-immunized/activated B cells in the inflamed periodontium; which is observed on Day 3 both in "*P. gingivalis*.-enhanced" (group D) and "ligatures only" (group B) experimental periodontitis. Moreover, the imaging results showed that the fluorescence intensity in group D on day 5 was the highest among all the 4 groups, suggesting that the transferred antigen-specific B cells could last longer in gingival tissues (Fig. 3C). The average intensity of group D (5.36×107 ± 0.84×106 [p/s/cm^{2}sr] / [μW/cm^2]) was higher than that of the same group on day 3 (Fig. 3C, 3D). It could lead to a reasonable speculation that the transferred antigen-specific B cells could be efficiently recruited into the inflammation sites in the presence of antigen. Although there is a significant difference in fluorescence intensity on day 5 among different groups, the intensity of fluorescence on day 10 in each group could be barely detected and was almost as low as those on day 0. No statistical difference was found among the 4 groups at day 10 (Fig. 3C, 3D), indicating that all the transferred B cells, whether from pre-immunized or non-immunized animals, were exhausted in gingival tissue on day 10 (Fig. 3C, 3D).

The number of gingival IL-10-expressing cells and CD19+ B cells was significantly higher in *P. gingivalis* ligation + pre-immunized B cells group than all other groups.

To determine the level of gingival IL-10 expression and CD19+ B cell infiltration *in situ*, immunohistochemical (IHC) staining was performed to locate the B cells and evaluate cytokine production in gingival tissues of all 4 groups of animals (Fig. 4A). The number of IL-10-expressing cells was significantly increased in *P. gingivalis* ligation + pre-immunized

Author Manuscript Author Manuscript Author Manuscript Author Manuscript

B cells group (group D) compared with ligation + non-immunized B cells group (group A), ligation + pre-immunized B cells group (group B) and *P. gingivalis* ligation + non-immunized B cells group (group C) (Fig. 4B), indicating that IL-10 expression was significantly increased by transfer of antigen-specific B cells. Moreover, gingival CD19 positive B cells were determined in all 4 groups (Fig. 4C). The data showed that the number of CD19 positive B cells was significantly increased in *P. gingivalis* ligation + pre-immunized B cells group (group D) compared with ligation + non-immunized B cells group (group A), ligation + pre-immunized B cells group (group B) and *P. gingivalis* ligation + non-immunized B cells group (group C) (Fig.4D).

Gingival IL-10 mRNA expression was significantly increased while TNF-α, IL-6, RANKL/OPG mRNA expressions were decreased in *P. gingivalis* ligation + pre-immunized B cells group compared with *P. gingivalis* ligation + non-immunized B cells group.

The gene expressions of pro-inflammatory cytokines (TNF-α , IL-1β, IL-6), anti-inflammatory cytokine (IL-10) and bone metabolism factor (RANKL, OPG) were detected using RT-qPCR. Gingival expressions of TNF-α (Fig. 5A) , IL-1β (Fig. 5B), IL-10 (Fig.5C), RANKL/OPG (Fig. 5D) and IL-6 (Fig. 5E) showed no significant differences when comparing ligation + non-immunized B cells group (group A) with ligation + pre-immunized B cells group (group B), suggesting that without the presence of antigen in gingival tissues there were no difference in inflammation and osteoclastogenesis effect after transfer of non-immunized or pre-immunized B cells. However, gingival expressions of TNF-α (Fig. 5A) , IL-1β (Fig. 5B), RANKL/OPG ratio (Fig. 5D) and IL-6 (Fig. 5E) were significantly decreased in *P. gingivalis* ligation + pre-immunized B cells group (group D) when compared with *P. gingivalis* ligation + non-immunized B cells group (group C). Also, IL-10 expression was significantly increased in group D compared with group C (Fig. 5C), which is consistant with the IHC result of IL-10 staining (Fig. 4A, 4B). Taken together, the transfer of pre-immunized B cells significantly increased IL-10 expression and reduced pro-inflammatory cytokine expression in gingival tissues compared with transfer of non-immunized B cells under same conditions, indicating that antigen-specific B cell transfer (with enriched B10 population) can effectively suppress experimental periodontitis inflammation.

Bone loss was significantly decreased in *P. gingivalis* ligation + pre-immunized B cells group compared with ligation only + pre-immunized B cells group and *P. gingivalis* ligation + non-immunized B cells group.

Fourteen days after different treatments, the maxillae were harvested and bone loss was examined as decribed in methods. The bone loss area was significantly decreased in *P. gingivalis* ligation + pre-immunized B cells group (group D) when compared to ligation + pre-immunized B cells group (group B) or *P. gingivalis* ligation + non-immunized B cells group (group C) (Fig. 5F), suggesting that in the presence of antigen in gingival tissues the transfer of pre-immunized B cells (with enriched B10 population) suppressed experimental periodontitis bone loss.

Author Manuscript Author Manuscript Author Manuscript Author Manuscript

Discussion

In vivo tracking of cells is a cutting edge technology to develop and optimize cell therapy for treatment or replacement of diseased tissues via transplanted cells [20–22]. IVIS system combines 2D optical and 3D optical tomography in one platform and is widely used in inflammation, autoimmunity and cancer research [13, 17, 23, 24]. However, it has been a challenge to track adoptively transferred cells in live mice oral cavity in longitudinal studies due to the limitation of accessibility, sensitivity and specificity of signal detection. Our present study is the first time using IVIS on mouse oral disease for *in vivo* tracking of cells in gingival tissues. To trace the signal inside oral cavity, it is critical to put the animal in a proper stabilized position and reduce peripheral background signals (Fig. 2B, 2C). In this study, cells were labelled with VivoTrack 680, a near-infrared fluorescent agent instead of bioluminescence. The VivoTrack 680 signal was confirmed to be detectable at least 10 days after transfer (Fig. 2D, 3C) and allowed us to track the signal through the period of experimental periodontitis. However, it still needs to be addressed in the future study on how to make more specific, stronger and long-lasting bioluminescence or fluorescence signal in the oral cavity of mice for *in vivo* tracking of rare population of cells and the determination of their long term effect.

IL-10 is widely studied as an anti-inflammation cytokine of balancing the inflammation, autoimmunity and cancer researches [25–28]. However, as a rare population of B cells, it was questioned on how B10 cells act to suppress host immune response in oral inflammatory disease such as periodontitis. Our previous study indicated that “primed” by LPS and CpG, B10 cells significantly reduced inflammation and bone loss in experimental periodontitis with increased IL-10 expression in gingival tissues [9]. However, it is unclear whether the increased IL-10 secretion was directly derived from local infiltration of transferred B10 cells or indirectly by the systemic anti-inflammatory effect of B10 transfer. This question has yet to be answered due to the difficulty of monitoring the B cell trafficking. In our present study, data from fluorescently-labelled B10 cells transfer in experimental periodontitis indicated that IL-10 expression was increased by transferred B10 cells infiltrated to the diseased site and such migration was directed by antigen specificity. Specifically, compared with control group without *P. gingivalis* ligation or non-immunized B cell transfer, the transfer of pre-immunized antigen-specific B10 cells can secret much higher level of IL-10 and suppress inflammatory cytokine production at local site (Figs. 4 and 5). It is recognized that the contribution of endogenous IL-10 expression by recipient immune system was not excluded in this study. To further verify our findings, IL-10 knock-out mice could be used as recipient mice in B10 cell transfer experiment in the future studies. Moreover, the previous study has indicated the cognate interaction between B10 and Th2 cells can enhance IL-10 expression by B10 cells and promote anti-inflammatory response [29]. Our recent study also confirmed that IL-21 co-stimulation can boost IL-10 potency of B10 cells *in vitro* and inhibit periodontal inflammation *in vivo* [11]. Furthermore, it is recognized that the increased expression of IL-10 cannot be ascribed specifically to infiltrating B cells, based on the experimental approach, since other type of cells such as T cells and resolving macrophages (M1) cells can also produce IL-10. The potential interaction between B cells and macrophages in the regulation of inflammatory responses has been suggested [30]. In our

Author Manuscript Author Manuscript Author Manuscript Author Manuscript

opinion, the immune inflammation vs. resolution is controlled by the complex immune regulatory network involving multiple cellular components and their contributions are probably determined by the tissue specificity and the stage of inflammatory process.

It may be considered ideal to use B cell-deficient (μMT) mice for such B cell adoptive transfer study in order to determine the exogenous B cell function. However, μMT mice showed complete absence of Ab responses and impaired cell-mediated immune responses [31]. These mice also demonstrated alterations in the cytokine microenvironment and defect in immune tolerance [32]. It is our opinion that the adoptive transfer of B10 cells into immune competent mice represents a better model to assess the function of the transferred cells than into the immune compromised animals. With the appropriate labelling techniques and immunohistochemical detection of the transferred cells we could track and identify these B cells *in vivo* during the experimental periodontitis, which allowed us to evaluate the B10 cell function under physiological conditions.

Furthermore, at the termination of the experiments *P. gingivalis* were detected in the gingival tissues of both *P. gingivalis*–associated ligature-induced periodontitis group C and Group D confirming the *P. gingivalis* colonization in the periodontal tissue (Supplemental Figure. S1). Thus, antigen priming enhanced the antigen-directed infiltration of B cells when *P. gingivalis* is present in the gingival tissues in group C and group D (Figure 3B). Although it is speculated that the transferred antigen-specific B10 cells could be more efficiently recruited into the inflammation sites and they might exert a better anti-bacterial function in-situ, our data indicated that the number of *P. gingivalis* in the periodontal tissues is not changed in animals transferred with pre-immunized or non-immunized B cells (Supplemental Figure. S1), which may indicate that the predominant function of B10 cells are not anti-microbial but immune regulation, leading to the reduced inflammation and bone loss. This may produce additional benefit to the host, as it ameliorates sustained overly aggressive inflammatory responses to bacterial infection and immune-mediated bone resorption. While not affecting a specific bacterium, it is yet to be determined whether such B10-mediated regulation of inflammation has any impact on overall periodontal microbiota and dysbiosis.

Additionally, we have compared B cells treated with CpG and *P. gingivalis* LPS with untreated B cells, both from non-immunized donor mice, for their trafficking and local infiltration after transferring these cells into *P. gingivalis*–associated ligature-induced periodontitis recipient mice. The fluorescence signal was measured using IVIS system before B cell transfer, day 3, day 5 and day 10 after transfer accordingly. The results clearly indicated that recipient mice transferred with the non-treated or *in vitro* CpG + LPS activated B cells from non-immunized donor mice maintained comparable low level of B cell local infiltration (Fig. S2). This results further suggested that the observed local B10 cell infiltration in *P. gingivalis*-associated ligature-induced experimental periodontitis requires specific antigen priming, and non-specific *in vitro* activation and expansion of B10 cells alone is not sufficient to achieve such local migration.

Our interpretation of enhanced antigen-directed B cell infiltration is based on our data showing the increased percentage of *P. gingivalis*-binding B cells and elevated IL-10

Author Manuscript Author Manuscript Author Manuscript Author Manuscript

expression from *P. gingivalis* immunized B cell populations. However, due to the limitation of the number of experimental groups, we cannot rule out the additional contributory factors of enhanced migratory capacity of B cells after *P. gingivalis* immunization, such as increased response to chemokines such as CXCL13 as a result of the immunization with *P. gingivalis*, and/or of the *in vitro* activation of B cells leading to the upregulation of CXCR5 expression on B cells before the transfer [33]. Future studies are warranted to determine if the enhanced B cell infiltration is also facilitated by the response to specific cytokines and chemokines.

In summary, the present study provided a novel model strategy to study function of immune cells in periodontitis through *in vivo* tracking of labeled cells in periodontium. The data indicated that antigen specificity dictate the local infiltration of B10 cells into periodontal tissue and promote anti-inflammatory responses and amelioration of periodontal bone resorption.

Supplementary Material

Refer to Web version on PubMed Central for supplementary material.

Funding

This study was supported by NIH NIDCR R01DE025255 and the Forsyth Institute FPILOT36 to X Han, and the Forsyth Institute FPILOT52 to Y Hu.

References:

[1]. Iwata Y, Matsushita T, Horikawa M, Dilillo DJ, Yanaba K, Venturi GM, Szabolcs PM, Bernstein SH, Magro CM, Williams AD, Hall RP, St Clair EW, Tedder TF, Characterization of a rare IL-10-competent B-cell subset in humans that parallels mouse regulatory B10 cells, Blood, 117 (2011) 530–541. [PubMed: 20962324]

[2]. Matsushita T, Tedder TF, Identifying regulatory B cells (B10 cells) that produce IL-10 in mice, Methods in molecular biology, 677 (2011) 99–111. [PubMed: 20941605]

[3]. Yanaba K, Yoshizaki A, Asano Y, Kadono T, Tedder TF, Sato S, IL-10-producing regulatory B10 cells inhibit intestinal injury in a mouse model, The American journal of pathology, 178 (2011) 735–743. [PubMed: 21281806]

[4]. Candando KM, Lykken JM, Tedder TF, B10 cell regulation of health and disease, Immunological reviews, 259 (2014) 259–272. [PubMed: 24712471]

[5]. Daien CI, Gailhac S, Mura T, Audo R, Combe B, Hahne M, Morel J, Regulatory B10 cells are decreased in patients with rheumatoid arthritis and are inversely correlated with disease activity, Arthritis & rheumatology, 66 (2014) 2037–2046. [PubMed: 24729478]

[6]. Han X, Lin X, Yu X, Lin J, Kawai T, LaRosa KB, Taubman MA, Porphyromonas gingivalis infection-associated periodontal bone resorption is dependent on receptor activator of NF-kappaB ligand, Infection and immunity, 81 (2013) 1502–1509. [PubMed: 23439308]

[7]. Hajishengallis G, Periodontitis: from microbial immune subversion to systemic inflammation, Nature reviews. Immunology, 15 (2015) 30–44.

[8]. Wang Y, Yu X, Lin J, Hu Y, Zhao Q, Kawai T, Taubman MA, Han X, B10 Cells Alleviate Periodontal Bone Loss in Experimental Periodontitis, Infection and immunity, 85 (2017).

[9]. Yu P, Hu Y, Liu Z, Kawai T, Taubman MA, Li W, Han X, Local Induction of B Cell Interleukin-10 Competency Alleviates Inflammation and Bone Loss in Ligature-Induced Experimental Periodontitis in Mice, Infection and immunity, 85 (2017).

[10]. Liu Z, Hu Y, Yu P, Lin M, Huang G, Kawai T, Taubman M, Wang Z, Xiaozhe H, Toll-like receptor agonists Porphyromonas gingivalis LPS and CpG differentially regulate IL-10

Author Manuscript Author Manuscript Author Manuscript Author Manuscript

competency and frequencies of mouse B10 cells, Journal of applied oral science : revista FOB, 25 (2017) 90–100. [PubMed: 28198981]

[11]. Hu Y, Yu P, Yu X, Hu X, Kawai T, Han X, IL-21/anti-Tim1/CD40 ligand promotes B10 activity in vitro and alleviates bone loss in experimental periodontitis in vivo, Biochimica et biophysica acta, (2017).

[12]. Imamura T, Saitou T, Kawakami R, In vivo optical imaging of cancer cell function and tumor microenvironment, Cancer science, 109 (2018) 912–918. [PubMed: 29465804]

[13]. Lim E, Modi KD, Kim J, In vivo bioluminescent imaging of mammary tumors using IVIS spectrum, Journal of visualized experiments : JoVE, (2009).

[14]. Trousil J, Ulmann V, Hruby M, Fluorescence & bioluminescence in the quest for imaging, probing & analysis of mycobacterial infections, Future microbiology, 13 (2018) 933–951. [PubMed: 29893148]

[15]. Diken M, Pektor S, Miederer M, Harnessing the potential of noninvasive in vivo preclinical imaging of the immune system: challenges and prospects, Nanomedicine, 11 (2016) 2711–2722. [PubMed: 27628499]

[16]. Nielsen MM, Schmidt JD, Christensen JP, Geisler C, Johansen JD, Bonefeld CM, Detection of local inflammation induced by repeated exposure to contact allergens by use of IVIS SpectrumCT analyses, Contact dermatitis, 76 (2017) 210–217. [PubMed: 28120518]

[17]. Sierakowiak A, Henriques-Normark B, Iovino F, IVIS Spectrum CT to Image the Progression of Pneumococcal Infections In Vivo, Methods in molecular biology, 1968 (2019) 195–202. [PubMed: 30929216]

[18]. Furukawa M, Sakakibara T, Itoh K, Kawamura K, Matsuura M, Kojima H, Suggestion of the updated IVIS cut-off values for identifying non-ocular irritants in the bovine corneal opacity and permeability (BCOP) assay, Toxicology in vitro : an international journal published in association with BIBRA, 45 (2017) 19–24. [PubMed: 28765095]

[19]. Ottobrini L, Lucignani G, Clerici M, Rescigno M, Assessing cell trafficking by noninvasive imaging techniques: applications in experimental tumor immunology, The quarterly journal of nuclear medicine and molecular imaging : official publication of the Italian Association of Nuclear Medicine, 49 (2005) 361–366.

[20]. Cao M, Mao J, Duan X, Lu L, Zhang F, Lin B, Chen M, Zheng C, Zhang X, Shen J, In vivo tracking of the tropism of mesenchymal stem cells to malignant gliomas using reporter gene-based MR imaging, International journal of cancer, 142 (2018) 1033–1046. [PubMed: 29047121]

[21]. Park BN, Lim TS, Yoon JK, An YS, In vivo tracking of intravenously injected mesenchymal stem cells in an Alzheimer's animal model, Cell transplantation, 27 (2018) 1203–1209. [PubMed: 30008224]

[22]. Uong TNT, Lee KH, Ahn SJ, Kim KW, Min JJ, Hyun H, Yoon MS, Real-Time Tracking of Ex Vivo-Expanded Natural Killer Cells Toward Human Triple-Negative Breast Cancers, Frontiers in immunology, 9 (2018) 825. [PubMed: 29770131]

[23]. Luli S, Di Paolo D, Perri P, Brignole C, Hill SJ, Brown H, Leslie J, Marshall HL, Wright MC, Mann DA, Ponzoni M, Oakley F, A new fluorescence-based optical imaging method to non-invasively monitor hepatic myofibroblasts in vivo, Journal of hepatology, 65 (2016) 75–83. [PubMed: 27067455]

[24]. Gutowski MB, Wilson L, Van Gelder RN, Pepple KL, In Vivo Bioluminescence Imaging for Longitudinal Monitoring of Inflammation in Animal Models of Uveitis, Investigative ophthalmology & visual science, 58 (2017) 1521–1528. [PubMed: 28278321]

[25]. Valsecchi C, Tagliacarne SC, Brambilla I, Klersy C, Benazzo M, Montagna L, Poddighe D, Ciprandi G, Marseglia GL, Licari A, Castellazzi A, Detection of IL10-producing B cell (B10) in adenoids of atopic children with adenoidal hypertrophy, Italian journal of pediatrics, 44 (2018) 30. [PubMed: 29486786]

[26]. Vera-Lozada G, Minnicelli C, Segges P, Stefanoff G, Kristcevic F, Ezpeleta J, Tapia E, Niedobitek G, Barros MHM, Hassan R, Interleukin 10 (IL10) proximal promoter polymorphisms beyond clinical response in classical Hodgkin lymphoma: Exploring the basis for the genetic control of the tumor microenvironment, Oncoimmunology, 7 (2018) e1389821. [PubMed: 29721365]

Author Manuscript Author Manuscript Author Manuscript Author Manuscript

[27]. Chen L, Shi Y, Zhu X, Guo W, Zhang M, Che Y, Tang L, Yang X, You Q, Liu Z, IL10 secreted by cancerassociated macrophages regulates proliferation and invasion in gastric cancer cells via cMet/STAT3 signaling, Oncology reports, 42 (2019) 595–604. [PubMed: 31233202]

[28]. Schmitt H, Ulmschneider J, Billmeier U, Vieth M, Scarozza P, Sonnewald S, Reid S, Atreya I, Rath T, Zundler S, Langheinrich M, Schuttler J, Hartmann A, Winkler T, Admyre C, Knittel T, Dieterich Johansson C, Zargari A, Neurath MF, Atreya R, The TLR9 agonist cobitolimod induces IL10 producing wound healing macrophages and regulatory T cells in ulcerative colitis, Journal of Crohn's & colitis, (2019).

[29]. Yoshizaki A, Miyagaki T, DiLillo DJ, Matsushita T, Horikawa M, Kountikov EI, Spolski R, Poe JC, Leonard WJ, Tedder TF, Regulatory B cells control T-cell autoimmunity through IL-21-dependent cognate interactions, Nature, 491 (2012) 264–268. [PubMed: 23064231]

[30]. Benard A, Sakwa I, Schierloh P, Colom A, Mercier I, Tailleux L, Jouneau L, Boudinot P, Al-Saati T, Lang R, Rehwinkel J, Loxton AG, Kaufmann SHE, Anton-Leberre V, O'Garra A, Sasiain MDC, Gicquel B, Fillatreau S, Neyrolles O, Hudrisier D, B Cells Producing Type I IFN Modulate Macrophage Polarization in Tuberculosis, American journal of respiratory and critical care medicine, 197 (2018) 801–813. [PubMed: 29161093]

[31]. Yang X, Brunham RC, Gene knockout B cell-deficient mice demonstrate that B cells play an important role in the initiation of T cell responses to Chlamydia trachomatis (mouse pneumonitis) lung infection, Journal of immunology, 161 (1998) 1439–1446.

[32]. Gonnella PA, Waldner HP, Weiner HL, B cell-deficient (mu MT) mice have alterations in the cytokine microenvironment of the gut-associated lymphoid tissue (GALT) and a defect in the low dose mechanism of oral tolerance, Journal of immunology, 166 (2001) 4456–4464.

[33]. Nakajima T, Amanuma R, Ueki-Maruyama K, Oda T, Honda T, Ito H, Yamazaki K, CXCL13 expression and follicular dendritic cells in relation to B-cell infiltration in periodontal disease tissues, Journal of periodontal research, 43 (2008) 635–641. [PubMed: 18624951]

Author Manuscript Author Manuscript Author Manuscript Author Manuscript

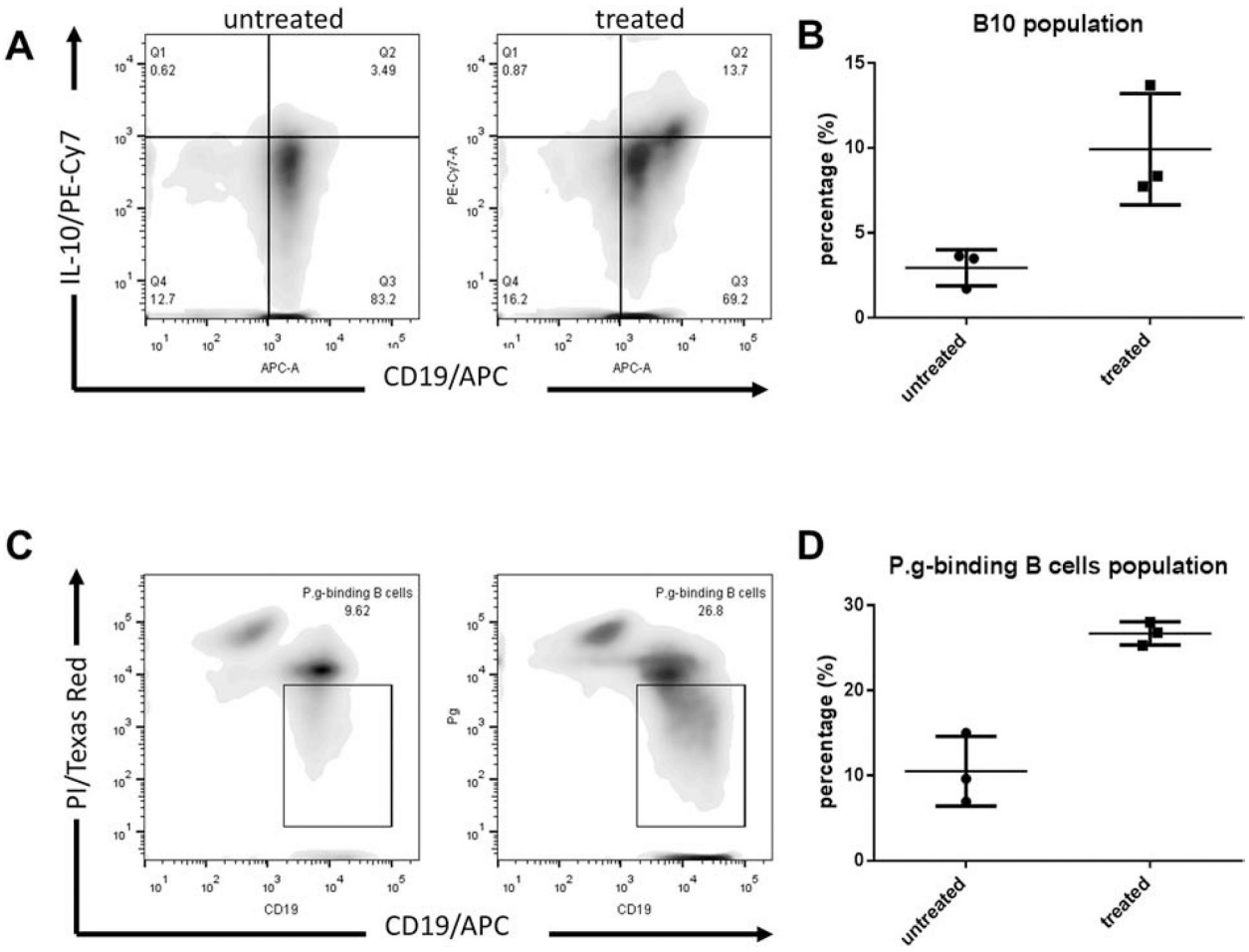

Figure 1. Populations of B10 cells and *P. gingivalis*-binding B cells increased after treatment with LPS and CpG *in-vitro*.

A. B10 cells were identified as $CD19^{+}IL\text{-}10^{+}$ in control (untreated group) and LPS + CpG treated group with flow cytometry analysis. **B**. The percentage of B10 cells were quantified (Mean ± SEM, n=3). **C.** *P. gingivalis* was labelled with the propidium iodide (PI) dye and antigen-specific (*P. gingivalis* binding) B cells were identified as $CD19^{hi}PI^{lo/int}$ in both groups with flow cytometry analysis (Mean ± SEM, n=3, $*p < 0.05$, $**p < 0.01$). **D**. The percentage of *P. gingivalis* binding B cells were quantified. (Mean ± SEM, n=3).

Author Manuscript Author Manuscript Author Manuscript Author Manuscript

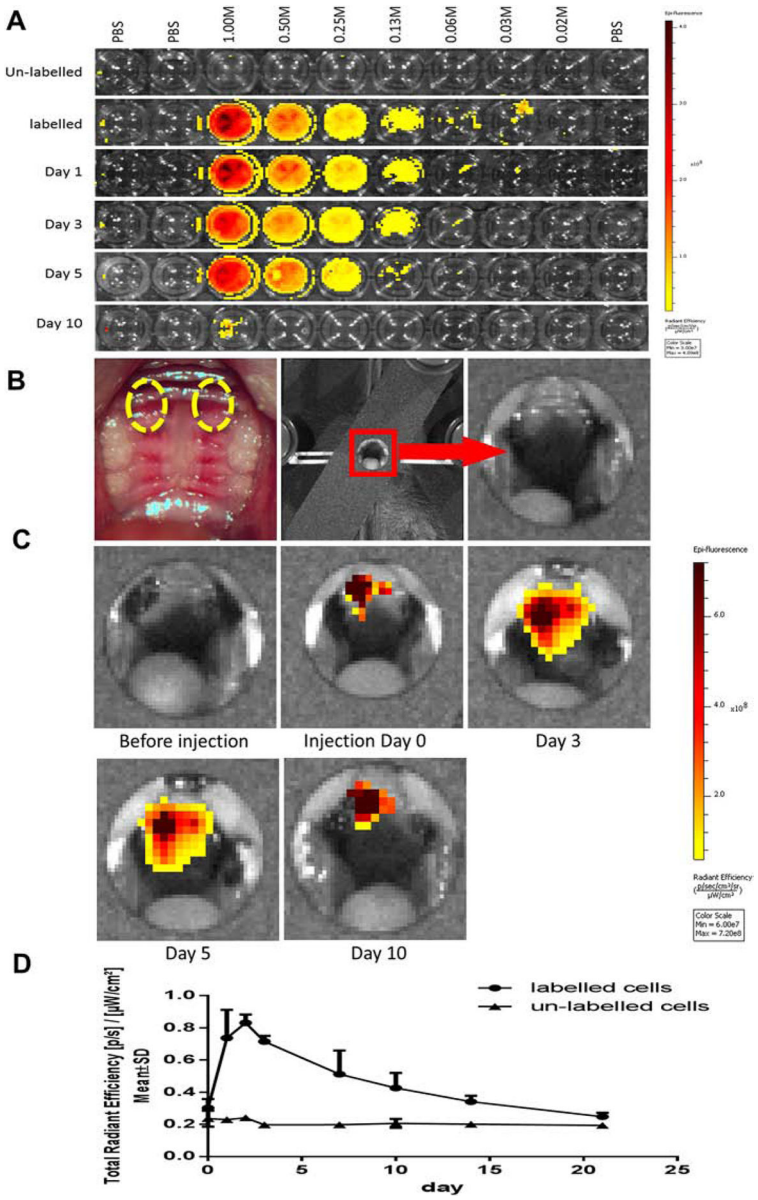

Figure 2. Fluorescence signal from labeled B cells could be detected and stable for 10 days both *in vitro* and *in vivo*.

A. The labelled cells were suspended in 100 μL of PBS on a 96-well plate, and were diluted with VivoTrack 680 solution in 1:2 ratio sequentially. **B**. The recipient mice (n=3 in each group) were used to receive the labelled or un-labelled B cells (10M in 100 μL of PBS) through tail vein injection. The fluorescence signal from the transferred cells in circulation could be detected for more than 20 days in vivo. **C**. Fluorescence signal of the labelled cells injected subgingivally in the palate could be detected for more than 10 days. The amount of injected cells was 1 M in 10 μL of PBS (right palate) or 0.1 M in 10 μL of PBS (left palate), respectively. The injection areas were indicated by the highlighted circles.

Author Manuscript Author Manuscript Author Manuscript Author Manuscript

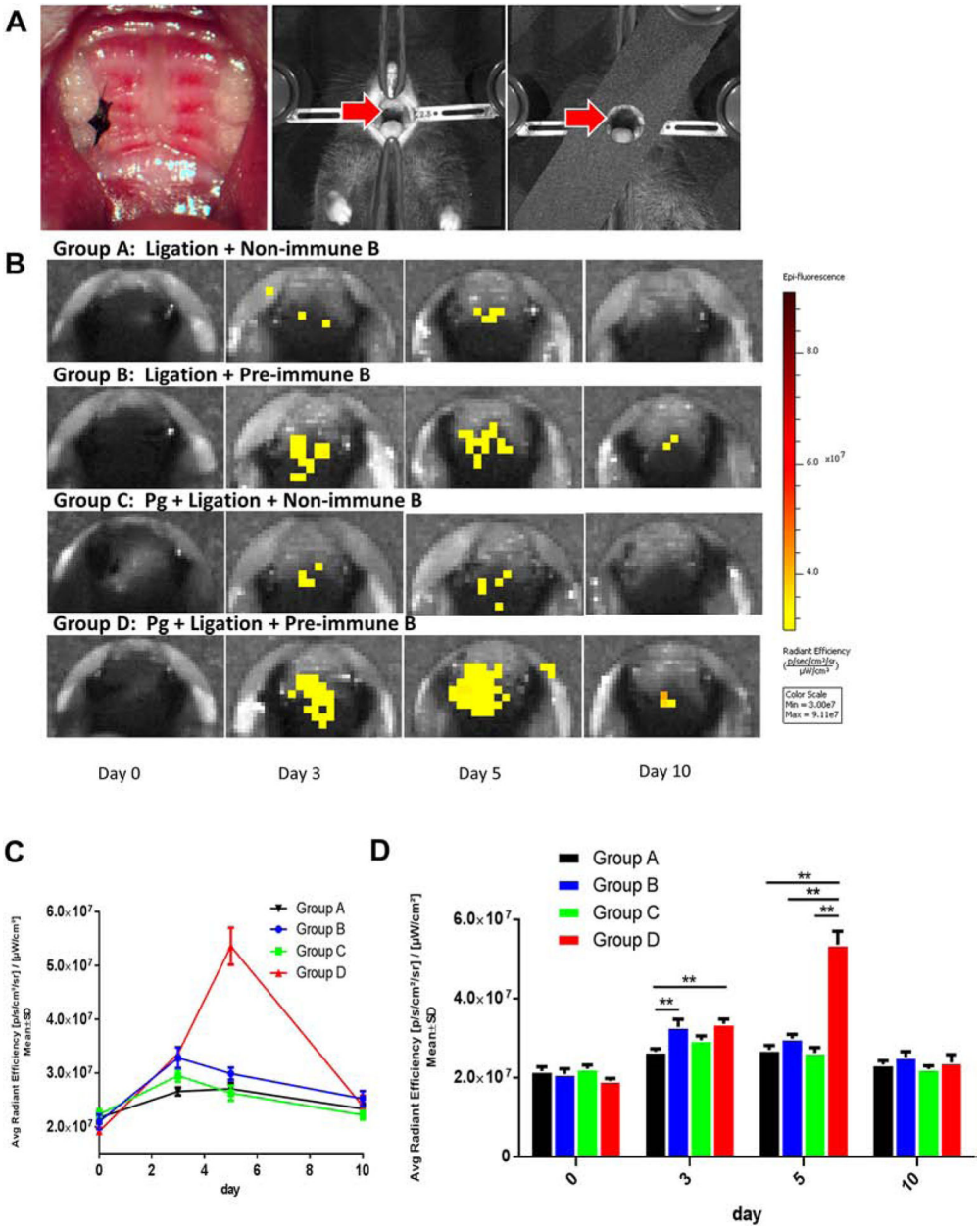

Figure 3. In-vivo imaging revealed antigen-directed gingival B10 infiltration in experimental periodontitis.

A. Silk ligature was placed around the right second maxillary molar and mice were positioned in acquisition platform in IVIS Spectrum *in vivo* imaging system. **B.** *In vivo* fluorescence showed that the antigen-specific B cells could be recruited more efficiently on day 3 in group B and D, comparing with that in group A and C, which were transferred with non-specific B cells. **C.** The level of fluorescence intensity showed a significant peak on day 5 in group D, comparing with the other 3 groups. **D.** On day 3, the fluorescence of group D was significantly higher than that of group A and B. While on day 5, the fluorescence of group D was significantly higher than those of the other 3 groups. (Mean ± SEM, n=5, $*p < 0.05$, $**p < 0.01$)

Author Manuscript Author Manuscript Author Manuscript Author Manuscript

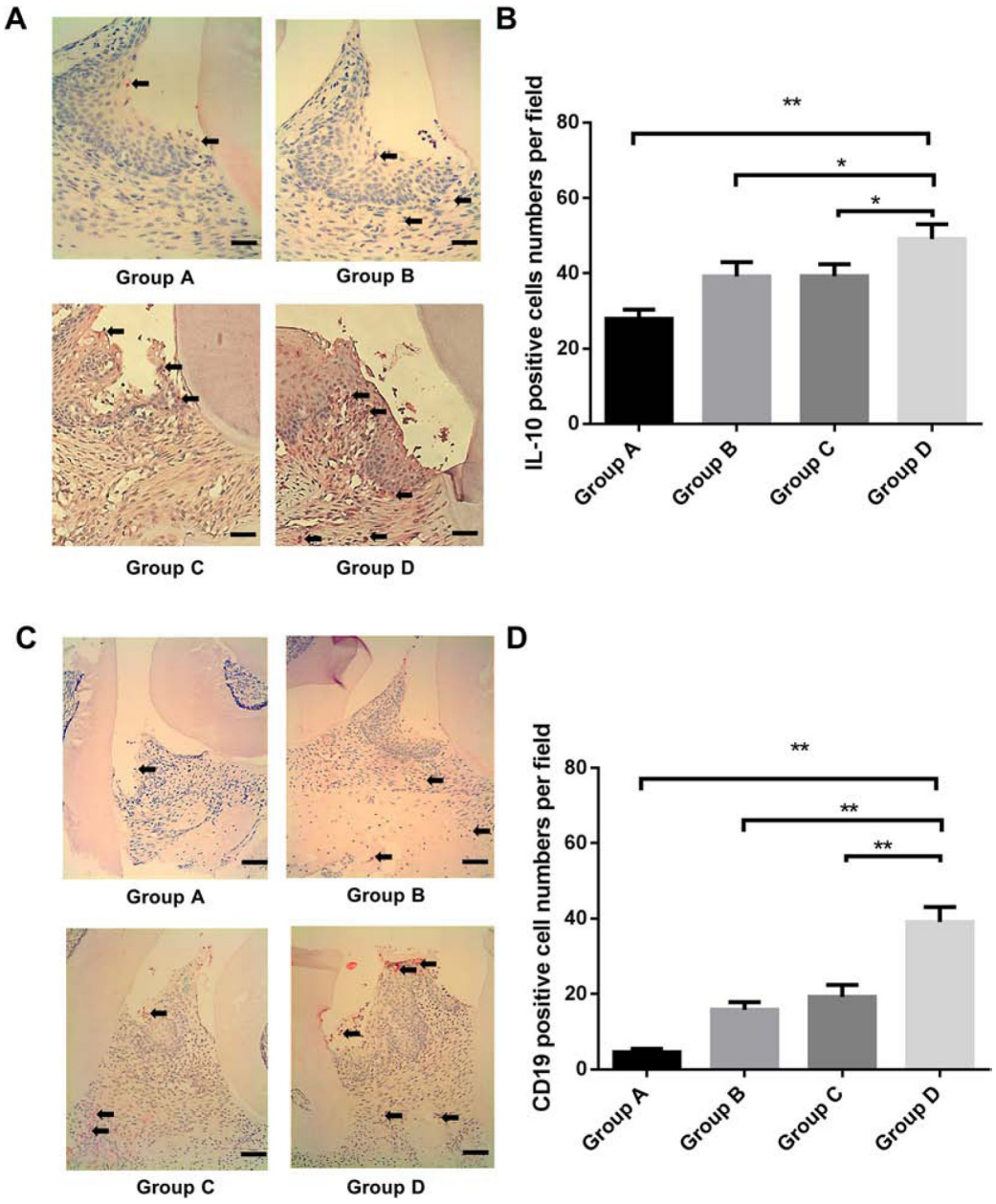

Figure 4. Gingival IL-10 expression levels in all experimental periodontitis groups.

A. Immunohistochemistry staining of IL-10 in the gingival tissue around ligation site were performed in Group A (ligation + non-immunized B cells), Group B (ligation + pre-immunized B cells), Group C (*P. gingivalis* ligation + non-immunized B cells) and Group D (*P. gingivalis* ligation + pre-immunized B cells) (Scale bar, 100 μm). **B**, the IL-10 positive cell numbers per field was analyzed and compared between groups. (Mean ± SEM, n=5, $*p < 0.05$, $**p < 0.01$). **C**. Immunohistochemistry staining of CD19 positive cells in the gingival tissue around ligation site were performed in Group A, B, C, and D. (Scale bar, 200 μm). **D**, The CD19 positive cell numbers per field was analyzed and compared between groups. (Mean ± SEM, n=5, $**p < 0.01$).

Author Manuscript Author Manuscript Author Manuscript Author Manuscript

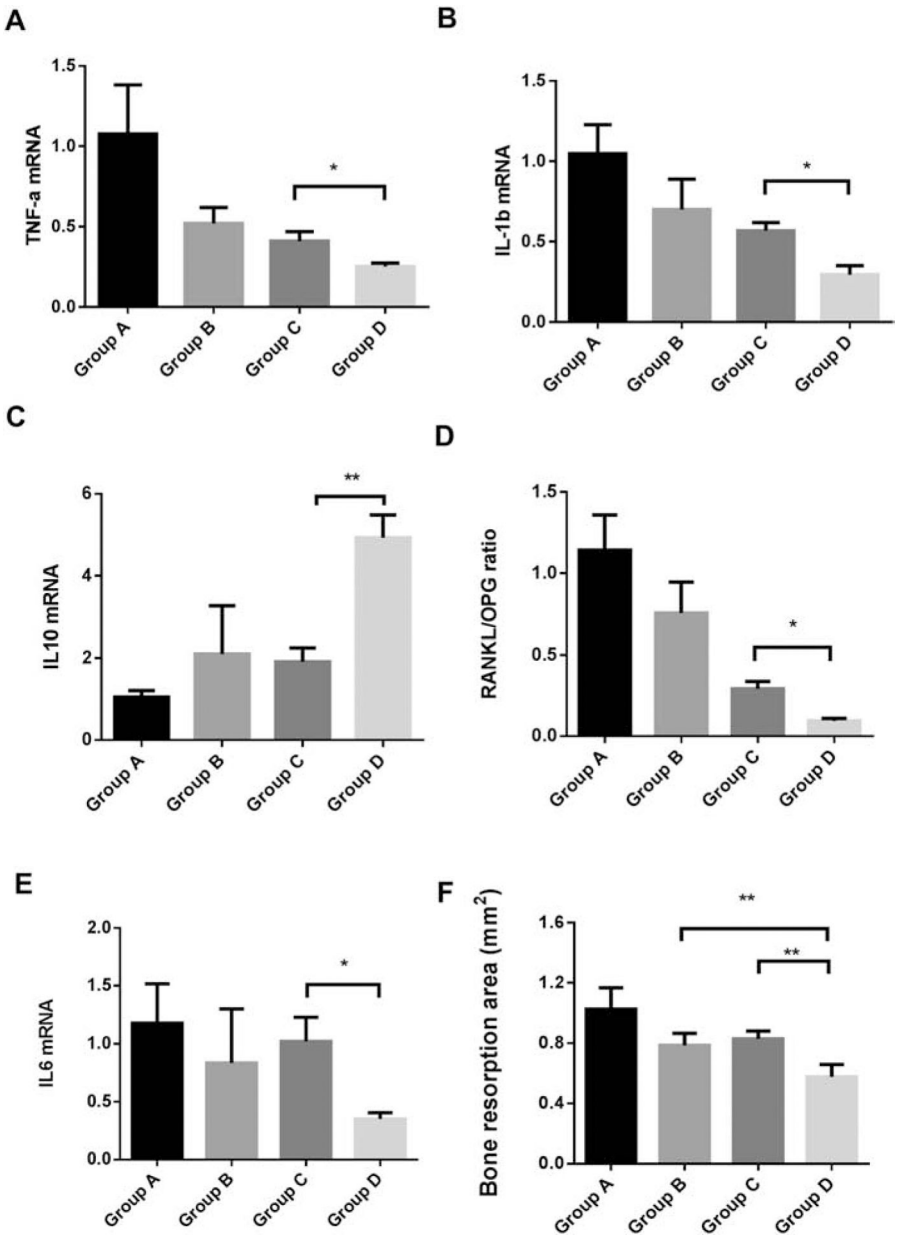

Figure 5. Gingival pro-inflammatory and anti-inflammatory cytokines mRNA expression changes and bone loss in all experimental periodontitis groups.

Gingival tissues around ligatured site were excised and processed for RT-qPCR analyses to determine mRNA level of **A.**TNF-α, **B.** IL-1β, **C.** IL-10, **D.** RANKL/OPG ratio, and **E.** IL-6 (Mean ± SEM, n = 5, *$p < 0.05$, **$p < 0.01$). **F**. Bone morphology was analyzed and quantified by Image J software using the pictures taken from maxilla bone 14 days after treatment in different groups. Data were presented as bone loss area in mm^2. (Mean ± SEM, n = 6, **$p < 0.01$)